1 **Gasoline aromatic: a critical determinant of urban secondary organic aerosol**
2 **formation**

4 Jianfei Peng[1,†], Min Hu[1, 4*], Zhuofei Du[1], Yinhui Wang[2], Jing Zheng[1], Wenbin Zhang[2],
5 Yudong Yang[1], Yanhong Qin[1], Rong Zheng[2], Yao Xiao[1], Yusheng Wu[1], Sihua Lu[1], Zhijun
6 Wu[1], Song Guo[1], Hongjun Mao[3], Shijin Shuai[2,*]

8 [1] State Key Joint Laboratory of Environmental Simulation and Pollution Control, College of
9 Environmental Sciences and Engineering, Peking University, Beijing 100871, China
10 [2] State Key Laboratory of Automotive Safety and Energy, Tsinghua University, Beijing
11 100084, China
12 [3] College of Environmental Sciences and Engineering, Nankai University, Tianjin 300071,
13 China
14 [4] Beijing Innovation Center for Engineering Science and Advanced Technology, Peking
15 University, Beijing 100871, China
16 [†] Now at Department of Atmospheric Sciences, Texas A&M University, College Station, TX
17 77843, US

18 [*]Corresponding author: Min Hu, minhu@pku.edu.cn; Shijin Shuai, sjshuai@tsinghua.edu.cn

19 **Abstract**

20 Gasoline vehicle exhaust is an important contributor to secondary organic aerosol (SOA)
21 formation in urban atmosphere. Fuel composition has potentially considerable impact on
22 gasoline SOA production, but the link between fuel components and SOA production is still
23 poorly understood. Here, we present chamber experiments to investigate the impacts of
24 gasoline aromatic content on SOA production through chamber oxidation approach. A
25 significant amplification factor of 3 - 6 for SOA productions from gasoline exhausts is
26 observed as gasoline aromatic content rose from 29% to 37%. Considerably higher emission
27 of aromatic volatile organic compounds (VOCs) using high-aromatic fuel plays an essential
28 role in the SOA production enhancement, while the semi volatile organic compounds (e.g.,
29 gas-phase PAHs) may also contribute to the higher SOA production. Our findings indicate
30 that gasoline aromatics significantly influence ambient $PM_{2.5}$ concentration in urban area and
31 highlight that more stringent regulation on gasoline aromatic content will achieve unexpected
32 benefit on urban air quality.

33

34 **1 Introduction**

35   Fossil fuel-powered vehicles, an important source of NO_x, volatile organic compounds

36 (VOCs) and atmospheric particulate matter (PM), are always associated with the severe haze

37 events, human health risks and climate forcing, particularly in urban areas (Parrish and Zhu,

38 2009; Guo et al., 2014; Huang et al., 2014; Kumar et al., 2014; Liu et al., 2015a; Kelly and

39 Zhu, 2016; Peng et al., 2016b). Gasoline is the most widely used vehicle fuel and accounts for

40 the largest total transportation energy consumptions in many countries, e.g., U.S. and China

41 (NBSC, 2015; EIA, 2015). Among all the gasoline related PM components, secondary

42 organic aerosols (SOA) produced via atmospheric oxidation of VOC precursors in the exhaust

43 have been proved by chamber experiments as a large fraction, if not the largest, of gasoline

44 vehicular PM (Zervas et al., 1999; Jimenez et al., 2009; Gordon et al., 2014a; Jathar et al.,

45 2014; Platt et al., 2014; Liu et al., 2015b). Moreover, ambient measurement also demonstrated

46 that gasoline SOA were the largest source of vehicular carbonaceous PM in megacities such

47 as Los Angeles (Bahreini et al., 2012). However, although increasingly stringent gasoline fuel

48 standards, especially on sulfur content, have been upgraded in the past decades in many

49 countries to reduce the emissions, the impacts of fuel compositions on SOA production have

50 not sufficiently been taken into account in the current gasoline fuel standards. This deficiency

51 is mainly attributed to the poor understanding of the effects of fuel properties on the related

52 SOA formation, and may ultimately lead to a policy bias on the control of vehicle emission

53 regarding to the reduction of atmospheric pollution.

54 Aromatic hydrocarbons, unsaturated compounds with at least one benzene ring, account

55 for 20% - 40% v/v of gasoline fuel. Aromatic VOCs (i.e., toluene, xylenes and

56 trimethylbenzenes) react exclusively with the OH radical in the atmosphere, leading to the

57 formation of a variety of semi- or low-volatile species (e.g., benzoic acid) (Zhang et al., 2015;

58 Schwantes et al., 2017), which will partition onto existing particle and be recognized as

59 anthropogenic SOA. Therefore, the higher emission of aromatic VOCs will likely result in

60 more SOA formation potential. Existing fuel-effect experimental and model studies have

61 shown that high-aromatic fuel in gasoline fuel will lead to more emissions of primary PM as

62 well as some aromatic VOCs (Zervas et al., 1999; EPA, 2013; Karavalakis et al., 2015; Wang

63 et al., 2016), indicating the considerable potential impact of gasoline aromatic content on

64 SOA production. Furthermore, though aromatic content in diesel fuel may have insignificant

65 impact on SOA formation (Gordon et al., 2014b), SOA production from gasoline vehicle is

66 considered more sensitive to aromatic content than that from diesel vehicle (Jathar et al.,

67 2013). However, until now, very few studies have successfully quantified the impact of

68 gasoline aromatic content on SOA production and directly revealed the possible pathway.

69   In this study, an in-depth comprehensive research was conducted to investigate the link

70 between gasoline fuel compositions, primary gas- and particle- phase emission, and

71 corresponding SOA formation. Gasoline exhaust emissions were examined on two platforms

72 under two different conditions. The first platform was the chassis dynamometer system

73 equipped with a constant volume sampler (CVS). Vehicle exhausts after CVS were

74 introduced into an outdoor environmental chamber and subjected to aging under typical

75 polluted urban conditions to simulate the SOA formation in ambient atmosphere. The second

76 platform was the experimental engine system on which emissions from a port gasoline

77 injection (PFI) engine and a gasoline direct injection (GDI) engine were examined. SOA

78 formation experiments from engine exhausts were carried out with relatively high OH

79 exposure compared to ambient conditions to obtain the SOA production potential. Most

80 importantly, different gasoline fuels blended from different refinery streams were utilized in

81 both platforms to probe the critical link among fuel components, VOCs emissions and related

82 SOA production.

83 **2 Materials and methods**

84 **2.1 Test fleet, cycle and engine.**

85   A commercial PFI vehicle, an experimental PFI engine and a GDI engine were tested in

86 this work.

87   The chosen PFI vehicle belonged to a commonly used vehicle model in China, which

88 certified to China IV emission standard (equivalent to Euro 4). The mileage of the test fleet

89 was about 3000 km. The fleet was driven on a chassis dynamometer system (Burke E. Porter

90 Machinery Company) using cold-start Beijing cycle in order to better simulate the actual

91 driving situation in Beijing. Beijing cycle was about 17 min long, with highest speed about 50

92 km h^{-1} (Fig. S1). The temperature and the absolute humidity in the dynamometer room were

93 kept at $23.0 \pm 1.0^{\circ}$ C and 8.4 ± 0.9 g m^{-3}, respectively, for all vehicle experiments (Table S1).

94   Vehicle exhaust underwent the first stage of dilution with filtered ambient air using a

95 constant volume sampler (CVS) operated at 5.5 m^3 min^{-1} for all experiments. Approximately

96 5.3 L min^{-1} of diluted exhaust from the CVS was introduced into the 1.2 m^3 chamber to be

97 further diluted with the clean air in the chamber (Fig. 1). The average dilution factor was

98 approximately 20 in the CVS and was approximately 15 in the chamber. During the entire

99 cycle, a light-duty gasoline vehicle emissions testing system (HORIBA, Ltd.) was used to

100 measure the average and real-time concentration of THC, CO_2, CO and NO_x. Besides, a filter

101 based sampler (AVL SPC 472) was used to sample primary particles from gasoline vehicles

102 for chemical composition analysis.

103 The PFI and GDI engines were manufactured by a domestic Chinese automaker and

104 equipped with turbocharger together with downsized displacement. The PFI engine used in

105 this study was an experimental one with an old three-way catalyst (TWC), while the GDI

106 engine was a commercial one designed for vehicles meeting the national IV emission standard.

107 The operation mode of the PFI and GDI engine for chamber experiments was 2000 round per

108 minute with 50% load. After the engine became stable at this operating mode, the exhaust was

109 introduced into the chamber passing through a heater (150°C) and a filter, with a flowrate of

110 5 L/min and an injection time of 1 min. Particle number, mass and chemical composition, as

111 well as VOCs in the exhaust were characterized at the same operating mode. Primary particles

112 were sampled by a filter based sampler (AVL SPC 472) and particulate chemical

113 compositions, i.e., ions, EC, OC and polar and nonpolar organic species, were analyzed using

114 ion chromatography, EC/OC analyzer (SUNSET Laboratory Inc.) and gas chromatography

115 mass spectrometry (GC-MS) (Guo et al., 2013), respectively. Detail description of the engine

116 experiments can be found in our previous study (Du et al., 2017) and all engine experiments

117 used in this study are illustrated in Table S2.

118 **2.2 Fuels**

119 Three fuels (F1, F2 and F3) were utilized in this study to investigate the impacts of the

120 gasoline fuel on SOA formation. A commercial Phase V gasoline (F1 fuel) with equivalent

121 octane number of 93 was used as the base fuel. F1 fuel contains 29.8% aromatics and 4.1%

122 olefin content (Table 1). The most abundant species in Fuel 1 was i-pentane, followed by

123 toluene and 2-methylpentane (Table S3).

124   F2 fuel was blended from 80% of F6 fuel and 20% of refinery catalytic stream. Octane

125   (18.8%) and aromatic content (28.5%) in F2 fuel are very similar with that in F1 fuel, with the

126   only difference to be the olefin content.

127   F3 fuel was blended from 80% of F2 fuel, 15–20% of refinery reformate stream with

128   high aromatic content and very small amount of o-octane and n-heptane to keep the same

129   octane level. Compared with F2 fuel, F3 fuel contained similar olefin content (15.4%) but

130   higher aromatic content (36.7%) (Table 1). In particular, much higher toluene, ethylbenzene

131   and methylethylbenzene were found in F3 fuel (Table S3). Both F2 and F3 fuels meet the

132   Phase V gasoline standard. On the basis of the aromatic contents, the F2 and F3 fuel can be

133   well representative of the fuel normally used in the year around 2010 and after 2013,

134   respectively, in Chinese market such as Beijing and Shanghai.

135   **2.3 Chamber Simulation**

136   The quasi-atmospheric aerosol evolution study (QUALITY) chamber was utilized to

137   quantify SOA formation from both gasoline engine exhaust and gasoline vehicle exhaust. The

138   1.2 m^3 two-layer chamber composed of an inner layer of 0.13 mm PFA Teflon and an outer

139   rigid 5.6 mm thick acrylic shell (Cyro Industries Acrylite, OP-4). Both layers allowed for

140   efficient transmission of sunlight in UV ranges (Peng et al., 2016b). Pre-experiments showed

141   that wall loss decreased the particle number concentration by about 50% in about 3.5 hours.

142   SO_2 and NO_x decreased to about 50% after 20 hours, while toluene and isoprene did not show

143   obvious wall loss during a two-day experiment (Peng et al., 2017).

144   Prior to each experiment, the QUALITY chamber was covered with two layers of

145   anti-UV cloth to shield the chamber from sunlight and flushed by zero air with a flowrate of

146   10 L min^{-1} for more than 15 hours to ensure a clean condition. In both vehicle and engine

147   experiments, excess (1 ml, 30% v/v) H_2O_2 was also injected into the chamber via the makeup

148   zero air as an extra hydroxyl radical (OH) source after adding the exhaust. Chamber

149   experiments were normally conducted from noon to later afternoon, with inside temperature

150   of 30 - 35 °C and relative humidity (RH) of 40 - 60%. A suite of high time resolution

151   state-of-the-art aerosol instruments were utilized to measure the gas concentration and a

152   comprehensive set of particle properties throughout the experiments, including concentrations

153 of HONO, SO_2, NO_x, O_3, CO, CO_2 and several VOCs, the particle diameter, mass, chemical

154 composition (Fig. 1 and Table S4).

155   Particle number distributions were measured with a scanning mobility particle sizer

156 (SMPS) system, which was composed by one differential mobility analyzer (DMA, TSI, Inc.,

157 model 3081) and one condensation particle counter (CPC, TSI, Inc., model 3772). The mass

158 concentration and size distribution of particle chemical compositions, including organic

159 aerosol (OA), sulfate, nitrate, ammonium and chloride, were measured by a high-resolution

160 time-of-flight aerosol mass spectrometer (HR-ToF-AMS, Aerodyne Research, Inc.). The

161 evolution of several VOCs was measured continually by a proton transfer reaction mass

162 spectrometer (PTR-MS, Ionicon HSL experiments). Dedicated gas monitors, including the

163 SO2, NOx, CO, CO_2 and O3 monitors (Thermo Inc.), were utilized, and calibrated each

164 experiment day. VOCs in the chamber were also sampled by canisters every 1 hour during

165 vehicle experiments and analyzed by GC-MS/FID system (Wang et al., 2015).

166   Zero airflow was connected to the chamber over the entire experiment to make up

167 volume of air withdrawn by the instruments. To minimize the sampling volume by the

168 instruments, all instruments except SMPS were connected with several three-way valves,

169 which were successively switched between the ambient air and the chamber very 15 or 30

170 min.

171 **3 Results**

172 **3.1 Simulation of SOA formation from gasoline exhausts.** The temporal evolution of gas-

173 and particle- phase species during the chamber experiment is illustrated in Figure 2. The

174 initial concentration of NO_x, benzene and toluene in the chamber were 163 ppb, 5.6 ppb and

175 16.8 ppb, respectively, corresponding to the severe urban haze condition in the megacities

176 (Guo et al., 2014). After the chamber was exposed to the sunlight, 99% of NO was converted

177 to NO_2 within the first 10 min. This is because the fast photolysis of H_2O_2 produced large

178 amount of OH radical and further HO_2/RO_2 radicals inside the chamber, which reacted with

179 NO to form NO_2 (Seinfeld and Pandis, 2006). Then, the concentration of O_3 increased rapidly

180 to approximately 400 ppb after 1 h exposure, and gradually decreased later in this experiment

181 (Fig.2a).

182   Over the entire experiment, benzene and toluene experienced gentle decay in the

183   concentrations, but with different decay coefficients (Fig. 2b). Aerosol evolution is always

184   characterized by a photochemical-age-based parameterization method in ambient

185   measurements as well as chamber experiments (Hu et al., 2013; de Gouw et al., 2005; Peng et

186   al., 2016a). Therefore, in order to compare our SOA productions in different experiments (in

187   which solar flux were different), OH exposures were calculated based on the ratios of benzene

188   and toluene concentrations, which reacted at different rates with OH radical (de Gouw et al.,

189   2005). Besides, to compare the OH exposure in our chamber experiments with the previous

190   ambient measurements, the OH concentration in the ambient air was assumed as 1.6×10^6

191   molec cm^{-3} (Hu et al., 2013; Peng et al., 2016a), and the equivalent photochemical ages of

192   chamber experiments were then estimated by the ratio of OH exposure in the chamber to the

193   assumed OH concentration in the ambient air.

194   New particle formation occurred inside the chamber within 10 min of exposure to the

195   sunlight (Fig. 2c). These newly formed particles performed as seeds for the further formation

196   of secondary species. A large quantity of secondary aerosols was then formed in the chamber,

197   leading to the fast growth in the diameter of these particles to approximately 70 nm after 3h

198   aging. The measurement of the particle compositions by the AMS reveals that the largest

199   mass fraction of secondary aerosols in the chamber was SOA (approximately 95%, Fig. S2),

200   indicating the critical role of the SOA for the secondary aerosol formation from gasoline

201   exhausts. Because of the low aerosol loading (initially lower than 2 μg m^{-3}) and low relative

202   humidity (40 - 50%) inside the chamber, heterogeneous reactions and aqueous phase

203   processing were not important for the formation of SOA in this study (Zhang et al., 2015).

204   Furthermore, the O:C ratio of SOA formed in the chamber stayed stable around 0.4 over the

205   entire experiment, indicating that condensed phase reactions, i.e., aqueous or heterogeneous

206   reactions, which produce highly oxidized oligomers, was not significant in the chamber

207   experiments in this study. These SOA, therefore, were likely formed via condensation of less

208   volatile products oxidized through gas phase reactions of VOCs precursors with limited

209   multigenerational chemistry (Robinson et al., 2007; Jimenez et al., 2009; Jathar et al., 2014).

210   The AMS spectrum profile of gasoline SOA obtained in this study was highly correlated with

211   the ambient low oxidized secondary organic aerosols (LO-OOA) in Beijing (R^2=0.99, Fig.

212   S3), further confirming the important contribution of gasoline emission on ambient PM$_{2.5}$.

213   SOA productions per fuel consumption or mileage were calculated on the basis of SOA

214   mass concentration inside the chamber, dilution factors both in the CVS and inside the

215   chamber, and fuel consumption/mileage of our working cycle. SOA mass concentration inside

216   the chamber was corrected according to the particle wall loss curve (Fig. S4) as well as the

217   dilution effect of both particles and gas precursors duo to the make-up zero air (Fig. S5). SOA

218   production at the end of this experiment was calculated to be 80 mg kg-fuel^{-1}, or 6.7 mg km^{-1}

219   after 3.5-hour aging (Fig. 2d). These values were 6.8 times higher than the emission factors

220   (EFs) of primary particles (including both primary organic matters and elemental carbon) at

221   the same cycle.

222   **3.2 Fuel impacts on SOA production.** The average fuel consumption per unit distance using

223   F1, F2 and F3 fuels were 0.113, 0.112 and 0.113 L km^{-1}, respectively, indicating no difference

224   in fuel economy among the three fuels. On the other hand, high-aromatic content gasoline led

225   to noticeably large enhancement on SOA production from both vehicle and engine

226   experiments. As illustrated in Figure 3a, the final SOA production from gasoline vehicle

227   exhaust ranged from 30 mg kg-fuel^{-1} to 98 mg kg-fuel^{-1} at the end of each experiment,

228   comparable to the results from cold start experiments in previous studies (Gordon et al.,

229   2014a; Jathar et al., 2014). Experiments using F3 fuel (with 36.7 % v/v aromatic content)

230   exhibit the highest SOA production factors, followed by F1 fuel (with 29.8 % v/v aromatics

231   content) and F2 fuel (with 28.5 % v/v aromatics content), successively. The average SOA

232   production at 12 equivalent photochemical-hours using F3 fuel was 76 mg kg-fuel^{-1} (6.3 mg

233   km^{-1}), equivalent to 3 times of that using F2 fuel (25 mg kg-fuel^{-1}, 2.1 mg km^{-1}). Additionally,

234   we observed much larger amount of the SOA formation in the first few photochemical hours

235   in all experiments. The average production rates of SOA were as high as 5 - 13 mg kg^{-1} h^{-1}

236   over each experiment, suggesting that the first-generation oxidation of some precursors inside

237   the chamber produced large amount of SOA. This indicated the existence of some

238   semi-volatile organic compounds (SVOCs) (Robinson et al., 2007; Keyte et al., 2013). It is

239   worth to mention that as the concentrations of gas pollutants and formed SOA in the chamber

240   using F3 fuel were 2-3 folders of those fusing F2 fuel, the partitioning of SVOCs in the

241   experiments using F3 fuel might slightly favor the SOA formation. This partitioning, however,

242   would not qualitatively change the experiment conclusion that higher fuel aromatics led to

243 higher SOA production.

244   SOA formation experiments from the PFI engine exhaust were conducted under high

245 oxidizing condition to obtain the SOA formation potential. As illustrated in Figure 3b, most

246 of the SOA were formed within the first half an hour of each engine experiment and very little

247 increase was observed over the following hours. The SOA formation potential from the

248 engine exhaust using F3 fuel was 3.3 g kg-fuel^{-1} at this condition, equivalent to 5.8 times of

249 that using F2 fuel, which was 0.57 g kg-fuel^{-1} on average. The high emission of the

250 experimental PFI engine suggests that the results of engine experiments could represent the

251 SOA production from gasoline vehicles with higher emission factor. Therefore, our results

252 with two different experimental sets (vehicle and engine experiments) demonstrate the

253 applicability of the SOA formation enhancement using high-aromatic fuel for gasoline vehicle

254 with either high or low emission factor, at either representative cycle condition or steady-state

255 operating condition.

256   Though good reproducibility was found for SOA production using either F2 or F3 fuels,

257 there were inevitably several biases in the chamber simulation approach. For example, the

258 SOA production in both vehicle and engine experiments might be underestimated due to loss

259 of SVOC vapors to the chamber wall as well as the condensation of low organic vapor onto

260 the particles that already lost on the chamber wall (Zhang et al., 2014). Also, the SOA

261 production in engine experiments could be overestimated because the high concentration in

262 the chamber might drive the gas-particle partitioning of the SVOCs into particle phase

263 (Robinson et al., 2007). Nevertheless, the relative enhancement factor of SOA for different

264 fuels was not largely influenced by these biases.

265 **3.3 Aromatic emission and SOA production.** To reveal the reason of this large

266 amplification on SOA production owing to fuel constitution, gasoline PM and VOC emissions

267 using F2 and F3 fuels were investigated (Fig. 4). Significant differences in the EFs among

268 different gas- and particle-phase species were observed. For example, the EFs of primary PM

269 in both number and mass concentration using F3 fuel were only 20% larger than those using

270 F2 fuel, consistent with previous studies (EPA, 2013; Karavalakis et al., 2015). Similar results

271 were also obtained for most of the alkane VOCs as well as NO. On the contrary, the EFs for

272 SOA, aromatic VOCs and particle-phase Polycyclic Aromatic Hydrocarbons (PAHs)

exhibited marked enhancement using high-aromatic gasoline fuel. The EFs of each aromatic VOCs from the exhaust experiment increased by a factor of 0.2 - 9.5 using high-aromatic gasoline fuel, with enhancement factors of 3.3 and 2.7 for total aromatic VOCs in vehicle and engine experiments, respectively (Fig. 4). Coincidentally, the total particle-phase PAHs emission was amplified for 1.8 times using high-aromatic gasoline fuel (F3 vs F2), with the amplification factor of each PAH species varied from 1.1 to 2.2. Since both gas-phase aromatic VOCs (one ring) and particle-phase PAHs (mostly 3-7 rings) exhibited much higher EFs using high-aromatic gasoline fuel, it is reasonable to speculate higher EFs of the semi-volatile PAHs (2-3 rings) in our experiments.

Aromatic components in the exhaust mainly come from two routes, which are the survival of fuel aromatic contents and the combustion-derived formation in the engine. Ethylene and acetylene are the key species for the combustion-derived aromatics. High concentrations of ethylene and acetylene accelerate the acetylene addition reaction, which generates light aromatic VOC as well as PAHs in the engine (Wang and Frenklach, 1997; Frenklach, 2002). In this study, when the high-aromatic fuel was used, the concentrations of ethylene and acetylene from GDI engine were enhanced by a factor of 3.3 and 2.7, respectively, indicating that more aromatics were formed through the addition reaction of acetylene and ethylene in the engine.

SOA production ($\Delta OA_{predicted}$) from VOC precursors in the exhaust was roughly estimated by multiplying the mass loss of each VOC precursors (Δi) by its SOA yield, Yi (Donahue et al., 2006):

$$\Delta OA_{predicted} = \sum_i (\Delta_i \times Y_i)$$

(1)

The SOA precursors here included benzene, toluene, C8-aromatics, C9-aromatics and styrene, which were all measured by PTR-MS during each experiment. The contributions of the alkenes and alkanes (7-11 carbons) to SOA formation in our experiments were also estimated using Eq. 1 based on the off-line GC-MS measurement. Results showed that the measured alkenes and alkanes (7-11 carbons) only accounted for approximately 4% of the total predicted SOA concentration (Fig. S6) duo to the low emission factors as well as the small

302 reacted proportion of these species inside the chamber. The yields of VOCi under high NOx

303 condition are used (Ng et al., 2007; Platt et al., 2013), due to the low initial VOCs/NOx ratios

304 which ranged from 0.5 to 1.0.

305   Figure 5 exhibits the two typical vehicle experiments with observed and predicted SOA

306 concentration as a function of photochemical age using F2 and F3 fuels, respectively. The

307 predicted SOA in the end of the two experiments accounted for 46% and 30% of the observed

308 SOA formation with toluene and C9-aromatics to be the largest contributors, consistent with

309 the previous results (Nordin et al., 2013; Platt et al., 2013; Gordon et al., 2014a). Predicted

310 SOA concentration using F3 fuel was about 90% higher than that using F2 fuel, suggesting

311 the import role of single-ring aromatic VOCs on the enhancement of SOA formation using

312 high-aromatic fuel. However, more than 50 % of the SOA concentration cannot be explained

313 by gas-phase oxidation of these single-ring aromatic VOCs. This value was even higher (up to

314 80%) in the first few photochemical hours in both experiments. Additionally, much larger

315 percentage of SOA using F3 fuel cannot be explained by the single-ring aromatic VOCs. This

316 suggests the existence of some unspeicated organic vapors, most likely SVOCs, which are

317 considered to have high SOA yield and might partition to particle phase after the

318 first-generation oxidation (Robinson et al., 2007; Chan et al., 2009; Jathar et al., 2014; Liu et

319 al., 2015b). Two-ring and three-ring PAHs, e.g., naphthalene and phenanthrene, which were

320 proved to have higher EFs using high-aromatic fuel (Chan et al., 2009), likely contributed

321 importantly to the SVOC vapors and might play a crucial role for the enhancement of SOA

322 production using high-aromatic fuel.

323 **4 Discussion**

324   Our results exhibit the critical impact of gasoline aromatics on urban SOA formation.

325 We observed an amplification factor of 3-6 on SOA formation using high-aromatic gasoline,

326 which was mainly caused by the high emission of one-ring aromatic VOCs as well as SVOC

327 such as gas-phase PAHs. This enhancement of SOA formation, meanwhile, was found using

328 not only a new vehicle meeting China IV emission standard, operated at a representative cycle

329 condition in Beijing, but also an experimental engine which emitted more gaseous pollutants

330 and was operated at steady state, suggesting the extensive applicability of our results.

331   Moreover, photo-oxidation of aromatics leads to significant production of small

332   dicarbonyls, i.e., glyoxal and methylglyoxal, which have high SOA yield via aqueous

333   reactions (Zhang et al., 2015). If this aqueous SOA pathway is taken account, the influence of

334   fuel on SOA formation will be much more remarkable. More work is needed to evaluate the

335   aqueous pathway of SOA formation from gasoline exhaust.

336   Currently, aromatic content in gasoline fuel is increasing continuously in China, where

337   more stringent standard on gasoline sulfur content has been upgraded and the oil refining

338   procedure are changing to meet the new standard. For example, we found the average

339   aromatic content for gasoline fuel in the market meeting Beijing Ⅲ, Ⅳ and Ⅴ standards

340   were 23.4%, 28.5% and 36.3%, respectively. Recent study found that gasoline aromatic

341   content in China was 9.6% higher than that in USA (Tang et al., 2015). Hence, the

342   enhancement in SOA formation exerted by the increase of aromatic content in gasoline fuel

343   from 29% to 37 % in this study can well represent the extra SOA formation due to the

344   gasoline standard change in Beijing. Neglect of this side effect of fuel standard change may

345   potentially offset the tremendous endeavors on vehicle emission control by the local

346   government. From another perspective, our findings provide a new direction in controlling air

347   pollution from vehicles, which is to decrease the aromatic content in the gasoline fuel. This

348   may require more hydrogenation catalysis process in the petroleum refining procedure instead

349   of catalytic reforming process, in which large amount of aromatic contents might be produced.

350   Compared with the vehicle restriction regulation that met the shrill opposition voice from the

351   society and the elimination of polluted vehicles that brought large amount of expenses, this

352   direction might be more acceptable, efficient and economical. Additionally, current vehicle

353   emission evaluation system, which mainly measures the emissions of PM, THC, NOx and CO,

354   will fail to tell the consequences of using the high-aromatic gasoline fuel, as these species do

355   not increase much when high-aromatic fuel is using (Fig. 4). Aromatic VOCs, especially the

356   SVOC, should be considered in future vehicle emission evaluation.

357   Furthermore, this influence of gasoline aromatic content on air quality is not only

358   adoptable in China. Strikingly, the current standard on gasoline aromatic content are not

359   stringent enough in most of the countries and regions in the world, where fuel standards with

360   very high maximum gasoline aromatic content (ranging from 35 % to 42% in different

361   countries, Table S6) are implemented, even including some developed countries and regions,

362 i.e., Europe, Japan, Australia. Our findings highlight the necessity of a more stringent

363 regulation on gasoline aromatic content in the next renewal of the gasoline standard.

364 **Acknowledgement**

365   This work was supported by the National Basic Research Program of China (973

366 Program) (2013CB228503, 2013CB228502, 2013CB955801); National Natural Science

367 Foundation of China (91544214, 51636003, 41421064); the Strategic Priority Research

368 Program of Chinese Academy of Sciences (XDB05010500); China Postdoctoral Science

369 Foundation (2015M580929). The authors thank Jianhua Xiao and Lei Deng in Tsinghua

370 University for their contribution to this work.

371

372 **References**

373 Bahreini, R., Middlebrook, A. M., de Gouw, J. A., Warneke, C., Trainer, M., Brock, C. A.,

374   Stark, H., Brown, S. S., Dube, W. P., Gilman, J. B., Hall, K., Holloway, J. S., Kuster, W.

375   C., Perring, A. E., Prevot, A. S. H., Schwarz, J. P., Spackman, J. R., Szidat, S., Wagner, N.

376   L., Weber, R. J., Zotter, P., and Parrish, D. D.: Gasoline emissions dominate over diesel in

377   formation of secondary organic aerosol mass, Geophys. Res. Lett., 39,

378   doi:10.1029/2011gl050718, 2012.

379 Chan, A. W. H., Kautzman, K. E., Chhabra, P. S., Surratt, J. D., Chan, M. N., Crounse, J. D.,

380   Kurten, A., Wennberg, P. O., Flagan, R. C., and Seinfeld, J. H.: Secondary organic aerosol

381   formation from photooxidation of naphthalene and alkylnaphthalenes: implications for

382   oxidation of intermediate volatility organic compounds (IVOCs), Atmos. Chem. Phys., 9,

383   3049-3060, doi:10.5194/acp-9-3049-2009, 2009.

384 de Gouw, J. A., Middlebrook, A. M., Warneke, C., Goldan, P. D., Kuster, W. C., Roberts, J.

385   M., Fehsenfeld, F. C., Worsnop, D. R., Canagaratna, M. R., Pszenny, A. A. P., Keene, W.

386   C., Marchewka, M., Bertman, S. B., and Bates, T. S.: Budget of organic carbon in a

387   polluted atmosphere: Results from the New England Air Quality Study in 2002, J.

388   Geophys. Res.-Atmos., 110, doi:10.1029/2004jd005623, 2005.

389 Donahue, N. M., Robinson, A. L., Stanier, C. O., and Pandis, S. N.: Coupled partitioning,

390   dilution, and chemical aging of semivolatile organics, Environ. Sci. Technol., 40,

391   2635-2643, doi:10.1021/es052297c, 2006.

392 Du, Z., Hu, M., Peng, J., Guo, S., Zheng, R., Zheng, J., Shang, D., Qin, Y., Niu, H., Li, M.,

393   Yang, Y., Lu, S., Wu, Y., Shao, M., and Shuai, S.: The Potential of Secondary Aerosol

394   Formation from Chinese Gasoline Engine Exhaust. *J. Environ. Sci.*, in press, 2017.

395 Energy Information Administration U.S. (EIA): October 2014 Monthly Energy Review,

396   DOE/EIA-0035(2014/10), http://www.eia.gov/totalenergy/data/monthly/pdf/mer.pdf,

397   2014.

398 Environmental Protection Agency U.S. (EPA): Assessing the Effect of Five Gasoline

399   Properties on Exhaust Emissions from Light-Duty Vehicles Certified to Tier 2 Standards:

400   Analysis of Data from EPAct Phase 3., EPA-420-R-13-002:232-233, 2013.

401 Frenklach, M.: Reaction mechanism of soot formation in flames, Phys. Chem. Chem. Phys., 4,

402   2028-2037, doi:10.1039/b110045a, 2002.

403 Gordon, T. D., Presto, A. A., May, A. A., Nguyen, N. T., Lipsky, E. M., Donahue, N. M.,

404   Gutierrez, A., Zhang, M., Maddox, C., Rieger, P., Chattopadhyay, S., Maldonado, H.,

405   Maricq, M. M., and Robinson, A. L.: Secondary organic aerosol formation exceeds

406   primary particulate matter emissions for light-duty gasoline vehicles, Atmos. Chem. and

407   Phys., 14, 4661-4678, doi:10.5194/acp-14-4661-2014, 2014a.

408 Gordon, T. D., Presto, A. A., Nguyen, N. T., Robertson, W. H., Na, K., Sahay, K. N., Zhang,

409   M., Maddox, C., Rieger, P., Chattopadhyay, S., Maldonado, H., Maricq, M. M., and

410   Robinson, A. L.: Secondary organic aerosol production from diesel vehicle exhaust:

411   impact of aftertreatment, fuel chemistry and driving cycle, Atmos. Chem. Phys., 14,

412   4643-4659, doi:10.5194/acp-14-4643-2014, 2014b.

413 Guo, S., Hu, M., Guo, Q., Zhang, X., Schauer, J. J., and Zhang, R.: Quantitative evaluation of

414   emission controls on primary and secondary organic aerosol sources during Beijing 2008

415   Olympics, Atmos. Chem. Phys., 13, 8303-8314, 2013.

416 Guo, S., Hu, M., Zamora, M. L., Peng, J. F., Shang, D. J., Zheng, J., Du, Z. F., Wu, Z., Shao,

417   M., Zeng, L. M., Molina, M. J., and Zhang, R. Y.: Elucidating severe urban haze

418   formation in China, P. Natl. Acad. Sci. U.S.A., 111, 17373-17378,

419   doi:10.1073/pnas.1419604111, 2014.

420 Hu, W. W., Hu, M., Yuan, B., Jimenez, J. L., Tang, Q., Peng, J. F., Hu, W., Shao, M., Wang,

421   M., Zeng, L. M., Wu, Y. S., Gong, Z. H., Huang, X. F., and He, L. Y.: Insights on organic

422   aerosol aging and the influence of coal combustion at a regional receptor site of central

423   eastern China, Atmos. Chem. Phys., 13, 10095-10112, doi:10.5194/acp-13-10095-2013,

424   2013.

425   Huang, R.-J., Zhang, Y., Bozzetti, C., Ho, K.-F., Cao, J.-J., Han, Y., Daellenbach, K. R.,

426   Slowik, J. G., Platt, S. M., Canonaco, F., Zotter, P., Wolf, R., Pieber, S. M., Bruns, E. A.,

427   Crippa, M., Ciarelli, G., Piazzalunga, A., Schwikowski, M., Abbaszade, G.,

428   Schnelle-Kreis, J., Zimmermann, R., An, Z., Szidat, S., Baltensperger, U., Haddad, I. E.,

429   and Prévôt, A. S. H.: High secondary aerosol contribution to particulate pollution during

430   haze events in China, Nature, doi:10.1038/nature13774, 2014.

431   Jathar, S. H., Miracolo, M. A., Tkacik, D. S., Donahue, N. M., Adams, P. J., and Robinson, A.

432   L.: Secondary Organic Aerosol Formation from Photo-Oxidation of Unburned Fuel:

433   Experimental Results and Implications for Aerosol Formation from Combustion

434   Emissions, Environ. Sci. Technol., 47, 12886-12893, doi:10.1021/es403445q, 2013.

435   Jathar, S. H., Gordon, T. D., Hennigan, C. J., Pye, H. O., Pouliot, G., Adams, P. J., Donahue,

436   N. M., and Robinson, A. L.: Unspeciated organic emissions from combustion sources and

437   their influence on the secondary organic aerosol budget in the United States, P. Natl. Acad.

438   Sci. U.S.A., 111, 10473-10478, doi:10.1073/pnas.1323740111, 2014.

439   Jimenez, J. L., Canagaratna, M. R., Donahue, N. M., Prevot, A. S. H., Zhang, Q., Kroll, J. H.,

440   DeCarlo, P. F., Allan, J. D., Coe, H., Ng, N. L., Aiken, A. C., Docherty, K. S., Ulbrich, I.

441   M., Grieshop, A. P., Robinson, A. L., Duplissy, J., Smith, J. D., Wilson, K. R., Lanz, V.

442   A., Hueglin, C., Sun, Y. L., Tian, J., Laaksonen, A., Raatikainen, T., Rautiainen, J.,

443   Vaattovaara, P., Ehn, M., Kulmala, M., Tomlinson, J. M., Collins, D. R., Cubison, M. J.,

444   Dunlea, J., Huffman, J. A., Onasch, T. B., Alfarra, M. R., Williams, P. I., Bower, K.,

445   Kondo, Y., Schneider, J., Drewnick, F., Borrmann, S., Weimer, S., Demerjian, K., Salcedo,

446   D., Cottrell, L., Griffin, R., Takami, A., Miyoshi, T., Hatakeyama, S., Shimono, A., Sun, J.

447   Y., Zhang, Y. M., Dzepina, K., Kimmel, J. R., Sueper, D., Jayne, J. T., Herndon, S. C.,

448   Trimborn, A. M., Williams, L. R., Wood, E. C., Middlebrook, A. M., Kolb, C. E.,

449   Baltensperger, U., and Worsnop, D. R.: Evolution of Organic Aerosols in the Atmosphere,

450   Science, 326, 1525-1529, doi:10.1126/science.1180353, 2009.

451   Karavalakis, G., Short, D., Vu, D., Russell, R., Hajbabaei, M., Asa-Awuku, A., and Durbin, T.

D.: Evaluating the Effects of Aromatics Content in Gasoline on Gaseous and Particulate Matter Emissions from SI-PFI and SIDI Vehicles, Environ. Sci. Technol., 49, 7021-7031, doi:10.1021/es5061726, 2015.

Kelly, F. J., and Zhu, T.: Transport solutions for cleaner air, Science, 352, 934-936, doi:10.1126/science.aaf3420, 2016.

Keyte, I. J., Harrison, R. M., and Lammel, G.: Chemical reactivity and long-range transport potential of polycyclic aromatic hydrocarbons - a review, Chem Soc Rev, 42, 9333-9391, 10.1039/c3cs60147a, 2013.

Kumar, P., Morawska, L., Birmili, W., Paasonen, P., Hu, M., Kulmala, M., Harrison, R. M., Norford, L., and Britter, R.: Ultrafine particles in cities, Environ. Int., 66, 1-10, doi:10.1016/j.envint2014.01.013, 2014.

Liu, S., Aiken, A. C., Gorkowski, K., Dubey, M. K., Cappa, C. D., Williams, L. R., Herndon, S. C., Massoli, P., Fortner, E. C., Chhabra, P. S., Brooks, W. A., Onasch, T. B., Jayne, J. T., Worsnop, D. R., China, S., Sharma, N., Mazzoleni, C., Xu, L., Ng, N. L., Liu, D., Allan, J. D., Lee, J. D., Fleming, Z. L., Mohr, C., Zotter, P., Szidat, S., and Prevot, A. S. H.: Enhanced light absorption by mixed source black and brown carbon particles in UK winter, Nat. Commun., 6, doi:10.1038/Ncomms9435, 2015a.

Liu, T., Wang, X., Deng, W., Hu, Q., Ding, X., Zhang, Y., He, Q., Zhang, Z., Lu, S., Bi, X., Chen, J., and Yu, J.: Secondary organic aerosol formation from photochemical aging of light-duty gasoline vehicle exhausts in a smog chamber, Atmos. Chem. Phys., 15, 9049-9062, doi:10.5194/acp-15-9049-2015, 2015b.

NBSC National Bureau of Statistics of China: China Statistical Yearbook, China Statistics Press, 2015.

Ng, N. L., Kroll, J. H., Chan, A. W. H., Chhabra, P. S., Flagan, R. C., and Seinfeld, J. H.: Secondary organic aerosol formation from m-xylene, toluene, and benzene, Atmos. Chem. Phys., 7, 3909-3922, 2007.

Nordin, E. Z., Eriksson, A. C., Roldin, P., Nilsson, P. T., Carlsson, J. E., Kajos, M. K., Hellén, H., Wittbom, C., Rissler, J., Löndahl, J., Swietlicki, E., Svenningsson, B., Bohgard, M., Kulmala, M., Hallquist, M., and Pagels, J. H.: Secondary organic aerosol formation from idling gasoline passenger vehicle emissions investigated in a smog chamber, Atmos.

482   Chem. Phys., 13, 6101-6116, doi:10.5194/acp-13-6101-2013, 2013.

483   Parrish, D. D., and Zhu, T.: Clean Air for Megacities, Science, 326, 674-675,

484   doi:10.1126/science.1176064, 2009.

485   Peng, J. F., Hu, M., Gong, Z. H., Tian, X. D., Wang, M., Zheng, J., Guo, Q. F., Cao, W., Lv,

486   W., Hu, W. W., Wu, Z. J., and Guo, S.: Evolution of secondary inorganic and organic

487   aerosols during transport: A case study at a regional receptor site, Environ. Pollut., 218,

488   794-803, doi:10.1016/j.envpol.2016.08.003, 2016a.

489   Peng, J. F., Hu, M., Guo, S., Du, Z. F., Zheng, J., Shang, D. J., Zamora, M. L., Zeng, L. M.,

490   Shao, M., Wu, Y. S., Zheng, J., Wang, Y., Glen, C. R., Collins, D. R., Molina, M. J., and

491   Zhang, R. Y.: Markedly enhanced absorption and direct radiative forcing of black carbon

492   under polluted urban environments, P. Natl. Acad. Sci. U.S.A., 113, 4266-4271,

493   doi:10.1073/pnas.1602310113, 2016b.

494   Peng, J., Hu, M., Guo, S., Du, Z., Shang, D., Zheng, J., Zheng, J., Zeng, L., Shao, M., Wu, Y.,

495   Colllins, D., and Zhang, R.: Aging and hygroscopicity variation of black carbon particles

496   in Beijing measured by a quasi-atmospheric aerosol evolution study (QUALITY) chamber,

497   Atmos. Chem. Phys. Discuss., https://doi.org/10.5194/acp-2017-370, in review, 2017.

498   Platt, S. M., El Haddad, I., Zardini, A. A., Clairotte, M., Astorga, C., Wolf, R., Slowik, J. G.,

499   Temime-Roussel, B., Marchand, N., Ježek, I., Drinovec, L., Močnik, G., Möhler, O.,

500   Richter, R., Barmet, P., Bianchi, F., Baltensperger, U., and Prévôt, A. S. H.: Secondary

501   organic aerosol formation from gasoline vehicle emissions in a new mobile environmental

502   reaction chamber, Atmos. Chem. Phys., 13, 9141-9158, doi:10.5194/acp-13-9141-2013,

503   2013.

504   Platt, S. M., El Haddad, I., Pieber, S. M., Huang, R. J., Zardini, A. A., Clairotte, M.,

505   Suarez-Bertoa, R., Barmet, P., Pfaffenberger, L., Wolf, R., Slowik, J. G., Fuller, S. J.,

506   Kalberer, M., Chirico, R., Dommen, J., Astorga, C., Zimmermann, R., Marchand, N.,

507   Hellebust, S., Temime-Roussel, B., Baltensperger, U., and Prevot, A. S. H.: Two-stroke

508   scooters are a dominant source of air pollution in many cities, Nat. Commun., 5,

509   doi:10.1038/Ncomms4749, 2014.

510   Robinson, A. L., Donahue, N. M., Shrivastava, M. K., Weitkamp, E. A., Sage, A. M.,

511   Grieshop, A. P., Lane, T. E., Pierce, J. R., and Pandis, S. N.: Rethinking Organic Aerosols:

Semivolatile Emissions and Photochemical Aging, Science, 315, 1259-1262, doi:10.1126/science.1133061, 2007.

Schwantes, R. H., Schilling, K. A., McVay, R. C., Lignell, H., Coggon, M. M., Zhang, X., Wennberg, P. O., and Seinfeld, J. H.: Formation of highly oxygenated low-volatility products from cresol oxidation, Atmos. Chem. Phys., 17, 3453-3474, 2017.

Seinfeld, J.H., and Pandis, S.N.: Atmospheric Chemistry and Physics: From Air Pollution to Climate Change, second ed. J. Wiley, New York, 2006.

Tang, G., Sun, J., Wu, F., Sun,Y., Zhu, X., Geng, Y. and Wang, Y.: Organic composition of gasoline and its potential effects on air pollution in North China. Sci. China Chem. 58(9), doi: 10.1007/s11426-015-5464-0, 2015.

Wang, H., and Frenklach, M.: A detailed kinetic modeling study of aromatics formation in laminar premixed acetylene and ethylene flames, Combust. Flame, 110, 173-221, doi:10.1016/S0010-2180(97)00068-0, 1997.

Wang, M., Shao, M., Chen, W., Lu, S., Liu, Y., Yuan, B., Zhang, Q., Zhang, Q., Chang, C. C., Wang, B., Zeng, L., Hu, M., Yang, Y., and Li, Y.: Trends of non-methane hydrocarbons (NMHC) emissions in Beijing during 2002-2013, Atmos. Chem. Phys., 15, 1489-1502, 2015.

Wang Y., Zheng, R., Qin, Y., Peng, J., Li, M., Xing, J., Wu, Y., Hu, M., and Shuai S..: The impact of fuel compositions on the particulate emissions of direct injection gasoline engine, Fuel, 166, 543-552, doi:10.1016/j.fuel.2015.11.019, 2016.

Yuan, B., Hu, W. W., Shao, M., Wang, M., Chen, W. T., Lu, S. H., Zeng, L. M., and Hu, M.: VOC emissions, evolutions and contributions to SOA formation at a receptor site in eastern China, Atmos. Chem. Phys., 13, 8815-8832, doi:10.5194/acp-13-8815-2013, 2013.

Zervas, E., Montagne, X., and Lahaye, J.: The influence of gasoline formulation on specific pollutant emissions, J. Air Waste. Manage., 49, 1304-1314, 1999.

Zhang, R., Wang, G., Guo, S., Zamora, M. L., Ying, Q., Lin, Y., Wang, W., Hu, M., and Wang, Y.: Formation of urban fine particulate matter, Chem. Rev., 115, 3803-3855, doi:10.1021/acs.chemrev.5b00067, 2015.

Zhang, X., Cappa, C. D., Jathar, S. H., Mcvay, R. C., Ensberg, J. J., Kleeman, M. J., and Seinfeld, J. H.: Influence of vapor wall loss in laboratory chambers on yields of secondary

542   organic   aerosol,   P.   Natl.   Acad.   Sci.   U.S.A.,   111,   5802-5807,

543   doi:10.1073/pnas.1404727111, 2014.

544

545   **Table 1**. Parameters of the tested fuels

546

Specifications	F1(BASE)	F2	F3
Ron	93.1	93.6	93
Mon	86.3	84.8	84
Density (g/ml)	0.72	0.728	0.744
Rvp (kpa)	58.6	63.2	55.4
Aromatics (%v/v)	29.8	28.5	36.7
Olefin (%v/v)	4.1	18.8	15.4
Ethanol (%v/v)	<0.1	0.12	0.01
Oxygen (%m/m)	0.01	0.06	0.02
Mn (mg/kg)	<0.1	<0.1	<0.1
Sulfur (mg/kg)	9	7	6
T10 (^{o}c)	50.8	50.9	55.4
T50 (^{o}c)	79.4	101.9	109.9
T90 (^{o}c)	162.6	167.5	164.3
Fbp (^{o}c)	187.9	195.7	194.4
Quality level	China Phase v	China Phase v	China Phase v

547
548

549
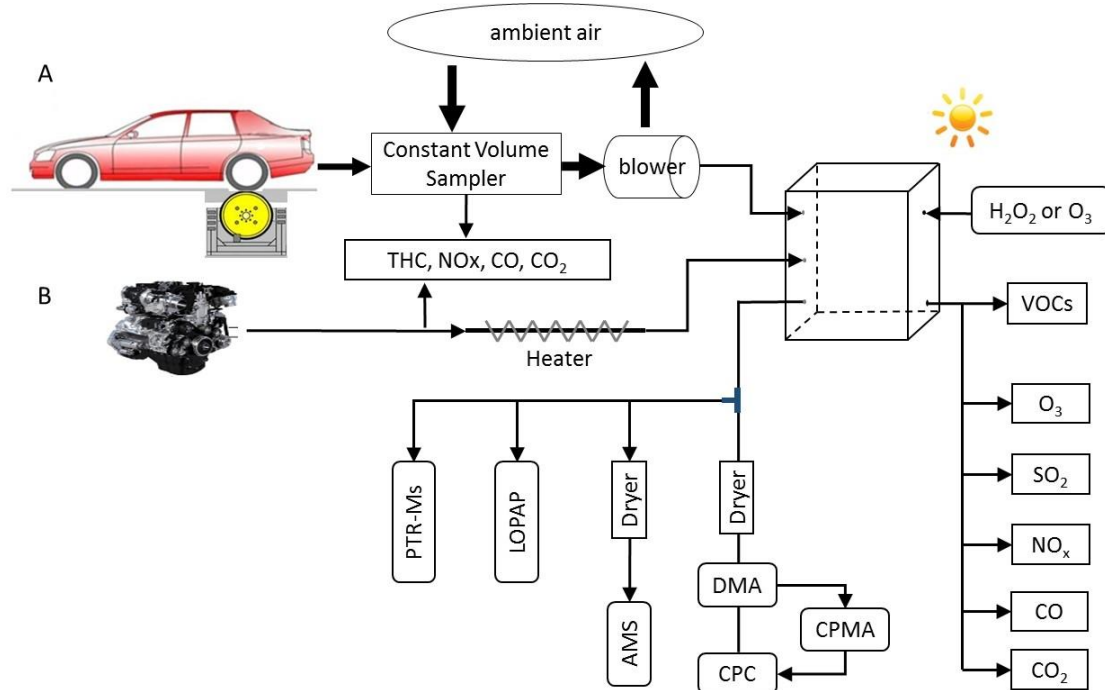
550

551 **Figure 1.** Schematic diagram of chamber experiments.

552
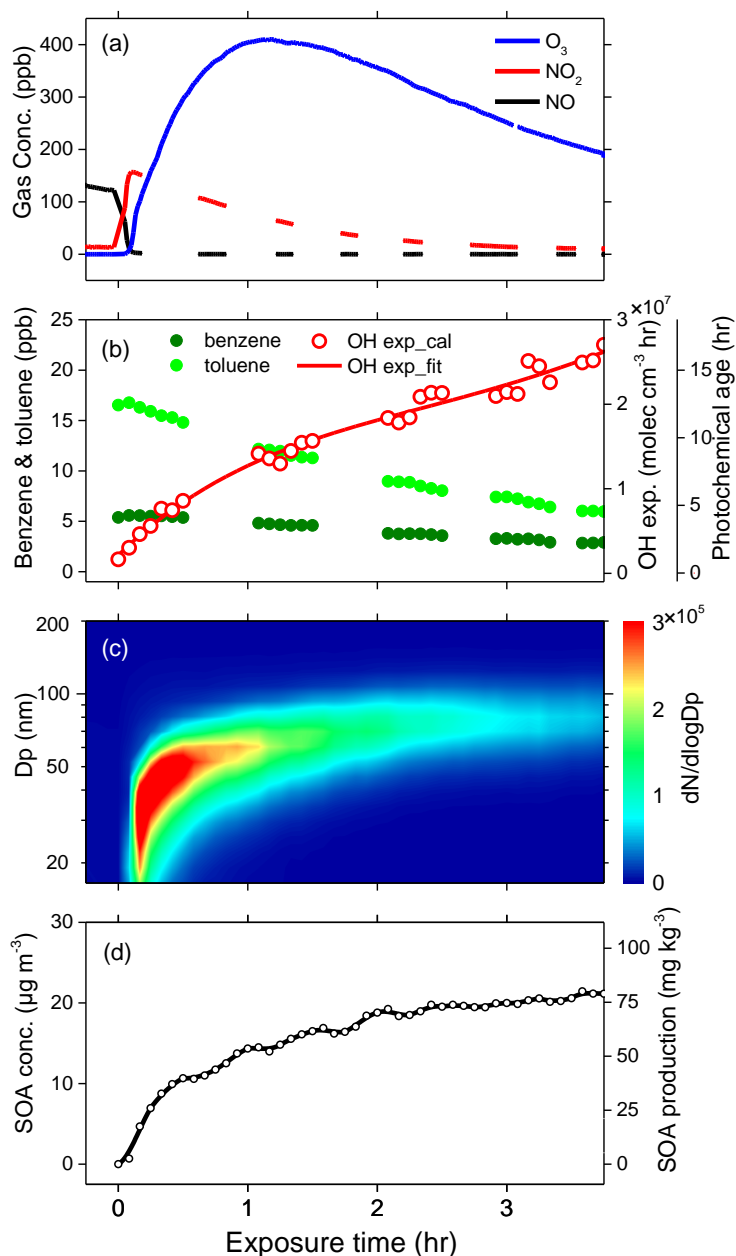
Figure 2. Evolution of gas-phase species (a, b), particle size distribution (c), and SOA concentration and production (d) during a typical chamber experiment (V2). OH exposure and photochemical age are calculated based on the ratios of benzene and toluene concentrations, assuming that OH concentration is 1.6×10^6 molec cm^{-3}. The SOA mass concentration is obtained by intergrading size distribution of particles inside the chamber on the basis of measured particle density. The measured SOA mass concentration is corrected according to the particle wall loss curve as well as the dilution effect for both particles and gas precursors.

562
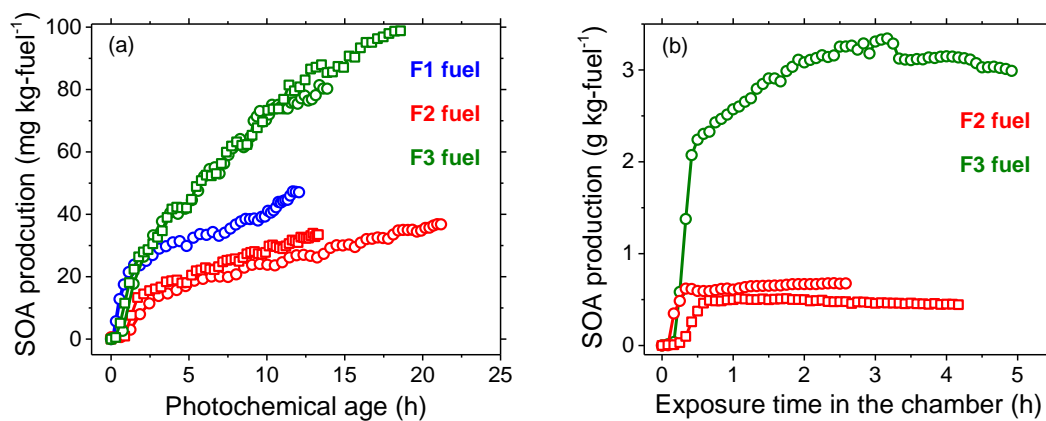
563

564 **Figure 3.** SOA production in the vehicle experiments as a function of photochemical age (a)

565 and in the engine exhaust experiments as a function of exposure time (b). The green squares,

566 green circles, red squares, red circles and blue circles (a) represent the experiment V1, V2, V3,

567 V4 and V5 shown in Table S1, respectively. The green circles, red squares and red circles (b)

568 represent the experiments E1, E2 and E3 shown in Table S2, respectively.

569

570

571
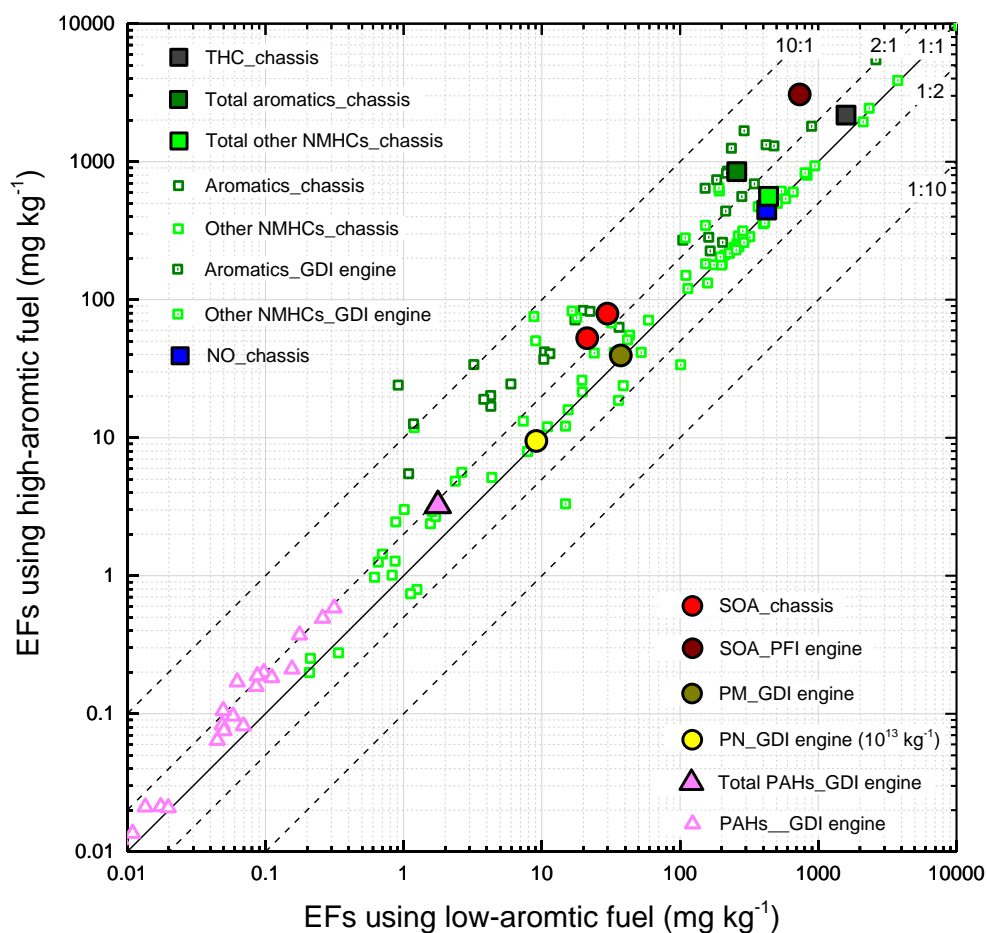
Figure 4. Comparison of emission factors (EFs) of gas- and particle species using high-aromatic fuel (F3 fuel) to those using low-aromatic fuel (F2 fuel). The total hydrocarbons (THC) were measured by vehicle emissions testing system, HORIBA, Ltd.), and the total aromatics and non-methane hydrocarbons (NMHCs) were measured by offline GC-MS. The black line denotes that the ratio of EFs using aromatic-rich fuel over aromatic-poor fuel is 1:1, and dashed lines stand for the ratios of 10:1, 2:1, 1:2, and 1:10, respectively. Note that the PAHs and VOCs data for the GDI engine were measured before the three-way Catalyst (TWC). Value in the figure can be found in Table S5.

580
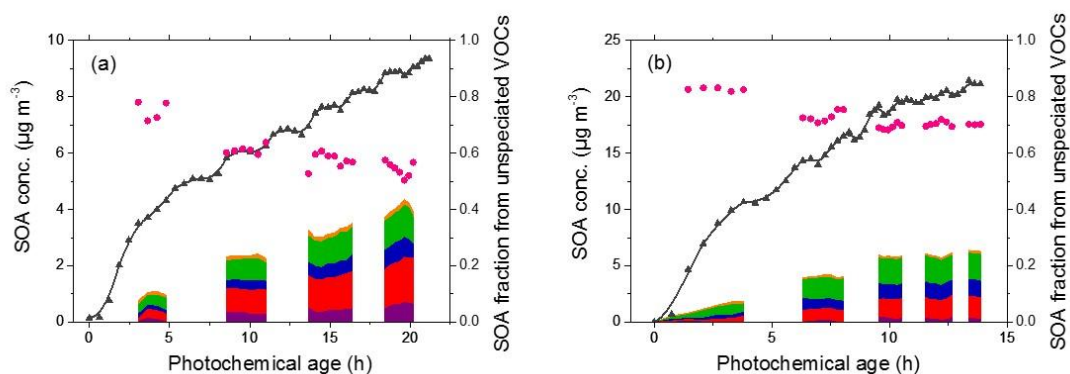
Figure 5. Observed and predicted SOA concentration, and SOA fraction from unspeciated VOCs as a function of photochemical age in typical chamber experiments using (a) F2 (experiment V4) and (b) F3 (experiment V2) fuels. Black line and triangles represent the corrected SOA concentrations in the chamber experiments. The purple, red, blue, green and yellow areas represent the predicted SOA from the oxidation of benzene, toluene, C8-aromatics, C9-aromatics and styrene, respectively. The pink circles represent the SOA fractions that cannot predicted by the one-ring aromatic VOC precursors.

588
589